ACS Sustainable Chemistry & Engineering

ACS AuthorChoice

Research Article

pubs.acs.org/journal/ascecg

Terms of Use

Comparison of Nonprecious Metal Cathode Materials for Methane Production by Electromethanogenesis

Michael Siegert,[†] Matthew D. Yates,[†] Douglas F. Call,[†,‡] Xiuping Zhu,[†] Alfred Spormann,[§] and Bruce E. Logan*[,†]

[†]Department of Civil and Environmental Engineering, The Pennsylvania State University, University Park, Pennsylvania 16802, United States

[‡]Department of Civil and Environmental Engineering, Syracuse University, Syracuse, New York 13244, United States

[§]Department of Civil and Environmental Engineering and Department of Chemical Engineering, Stanford University, Stanford, California 94305, United States

Supporting Information

ABSTRACT: In methanogenic microbial electrolysis cells (MMCs), CO_2 is reduced to methane using a methanogenic biofilm on the cathode by either direct electron transfer or evolved hydrogen. To optimize methane generation, we examined several cathode materials: plain graphite blocks, graphite blocks coated with carbon black or carbon black containing metals (platinum, stainless steel or nickel) or insoluble minerals (ferrihydrite, magnetite, iron sulfide, or molybdenum disulfide), and carbon fiber brushes. Assuming a stoichiometric ratio of hydrogen (abiotic):methane (biotic) of 4:1, methane production with platinum could be explained solely by hydrogen production. For most other materials, however, abiotic hydrogen production rates were insufficient to explain methane production. At −600 mV, platinum on carbon black had the highest abiotic hydrogen gas formation rate (1600 ± 200 nmol cm^{-3} d^{-1}) and the highest biotic methane production rate (250 ± 90 nmol cm^{-3} d^{-1}). At −550 mV, plain graphite (76 nmol cm^{-3} d^{-1}) performed similarly to platinum (73 nmol cm^{-3} d^{-1}). Coulombic recoveries, based on the measured current and evolved gas, were initially greater than 100% for all materials except platinum, suggesting that cathodic corrosion also contributed to electromethanogenic gas production.

KEYWORDS: *Biocathode, Carbon capturing and sequestration, Microbial electrolysis cell, Power-to-gas, Microbially influenced corrosion, Carbon black, Graphite, Polyacrylonitrile*

INTRODUCTION

The conversion of electrical current into transportable fuels offers an opportunity to both store energy as well as to provide it for other uses, such as transportation or chemical production. Low carbon content fuels are particularly of interest as they are relatively clean burning in combustion engines. Most electrochemical strategies for direct methane production from CO_2 require precious metals or copper to reduce electrical overpotentials, and the reactions are not sufficiently specific, resulting in production of undesired higher molecular weight alkanes and carbon products that can foul the electrodes.[1,2]

Combined biological and electrochemical methods for methane production show great promise as they are specific for production of a single product without the need for precious metals.[3] Methanogenic microorganisms can produce methane using only a limited number of organic molecules (e.g., acetate, formate, and methanol). However, some methanogens can reduce CO_2 using hydrogen gas, enabling methane production using only these two inorganic chemicals. Most methane is produced from fossil sources, but hydrogen gas produced through water electrolysis could alternatively be supplied to methanogens to make methane. However, hydrogen gas production by water electrolysis often requires expensive precious metals to reduce cathodic overpotentials. Biological methane production by direct electron transfer from a carbon electrode using microorganisms can provide a direct route of methane production from electrical current (electromethanogenesis), without the need to evolve hydrogen gas for hydrogenotrophic methanogenesis.[4]

The energy requirements for methane production by direct electron transfer to methanogens can theoretically be less than that needed via hydrogen gas due to the possibility of using lower set cathode overpotentials. Theoretically, hydrogen gas can be evolved under physiological standard conditions (pH 7, 1 M solute concentrations, and 1 atm for gases) at a potential of

Received: December 9, 2013
Revised: January 23, 2014
Published: February 18, 2014

−410 mV (eq 1) (vs a standard hydrogen electrode, SHE), based on

$$2H^+ + 2e^- \rightarrow H_2 \quad E = -410\ \text{mV} \tag{1}$$

Therefore, this is the minimum cathode potential needed for methane production via hydrogenotrophic methanogenesis under these conditions. Generation of methane from the reduction of CO_2 without H_2 generation can theoretically occur at a less negative cathode potential of −240 mV, based on the half-cell reaction of

$$CO_2 + 8H^+ + 8e^- \rightarrow CH_4 + 2H_2O \quad E = -240\ \text{mV} \tag{2}$$

This route requires microorganisms to consume electrons directly from the cathode. Because of kinetic limitations and imperfect electrode reactions, cathode potentials more negative than these theoretical values are applied to generate measurable production rates. Applied potentials used in previous electrochemical methane production studies, such as −650 mV[5] and −500 mV[4], allow for methane production by either direct electron transfer or via hydrogen gas. However, measured abiotic hydrogen gas production rates on electrodes lacking effective hydrogen gas catalysts, such as platinum, are generally insufficient to explain observed methane gas production rates, suggesting methane can be produced by direct electron transfer.[4] While it cannot be known for certain whether methane production occurred by direct electron transfer or by hydrogen gas production in these previous studies, from a process cost perspective knowing the exact route is less important than minimizing costs. In order to minimize operating costs for methane evolution, using more positive cathode potentials will reduce energy requirements. Avoiding the need for precious metals is also important to make the overall bioelectrochemical process more environmentally sustainable.

Biocathode overpotentials could be reduced by choosing materials that are optimized to improve direct electron transfer to methanogens or by using materials that efficiently catalyze hydrogen evolution at low potentials (without the need for precious metals). Materials that might be useful to reduce overpotentials for direct electron transfer could be those that are known to undergo microbially influenced corrosion by methanogens. For example, methane can be directly produced by microbial corrosion of zero-valent iron.[6,7] Although the exact mechanism(s) for this type of corrosion remain enigmatic, the process may require formation of an iron sulfide crust.[8] When steel corrodes, it becomes covered with an insoluble mineral crust consisting mainly of iron oxide and/or hydroxide ($Fe_xO_x[OH]_x$), and under sulfate-reducing conditions, this crust may also contain iron sulfides (Fe_xS_x). These minerals accelerate the process of corrosion as they are electrically conductive, and therefore, they facilitate release of electrons compared to pure iron.[9] Other materials that might be used for stimulating direct electron transfer to methanogens are semiconductive iron minerals like magnetite, as they have been shown to enhance interspecies electron transfer in methanogenic mixed cultures.[10] Ferrihydrite may also be useful. Although it has not been shown to be involved in interspecies electron transfer, it is known that the methanogen *Methanosarcina barkeri* can reduce ferrihydrite.[11] Nonprecious metals could be used to reduce cathode potentials and improve methane production via hydrogenotrophic methanogenesis. Iron sulfide (FeS) has been shown to decrease the electrical overpotential required for abiotic hydrogen formation compared with pure iron,[9] as has stainless steel,[12] nickel,[13] and molybdenum disulfide (MoS_2).[14] While metallic compounds can be protected from corrosion by cathodic potentials (cathodic protection), crystalline or amorphous compounds cannot.

Another strategy for facilitating bioelectrochemical methane production through reduced electrode overpotentials is using carbon materials with high surface areas, as long as all of the surface area is accessible to the microorganisms (i.e., not in pores smaller than the microbes). Examples of carbon materials previously used as cathodes in MMCs include graphite blocks,[4] granules,[15,16] and felt;[17] carbon felt;[18] carbon paper;[5] and carbon paper coated with carbon black (Vulcan XC-72R).[19] Cathodes made from these materials with high surface areas could enable overall efficient electron transfer even with low current densities per unit area.[20] Carbon materials also have good adhesion properties for methanogens.[21]

In order to improve methane production in MMCs, we tested different types of materials as alternatives to platinum: metal powders of stainless steel or nickel; iron mineral coatings of ferrihydrite, magnetite, or iron sulfide; MoS_2; and carbon-based materials that included plain graphite blocks, blocks coated with carbon black powder, and carbon fiber brushes. The rates of hydrogen gas evolution for each of these materials was examined prior to inoculation in abiotic reactors in order to better understand whether methane production in biotic reactors was mainly driven by hydrogen gas evolution or whether these materials could enhance electromethanogenesis. The total charge transferred (Coulombs) from the measured current was compared to the balance of electrons recovered in hydrogen and methane gas in order to determine if there was full recovery of current in the gas produced (Coulombic recoveries, CR <100%) or if corrosion was occurring (CR > 100%).

MATERIALS AND METHODS

Inoculum and Medium Composition. Anaerobic sludge from the secondary digester of Penn State's municipal wastewater treatment plant was used to inoculate the reactors (1% w/v). All procedures were carried out with strict oxygen exclusion using bottles with thick butyl rubber stoppers (Wheaton, Millville, NJ, U.S.A.). The medium used for all experiments was prepared from a 10× stock solution and contained (final concentration in g L^{-1}) $NaHCO_3$ 2.5, NH_4Cl 1.5, NaH_2PO_4 0.6, and KCl 0.1. Vitamins and trace elements (10 mL L^{-1} each; Supporting Information) were added after autoclaving and flushing the headspace of the hot medium with N_2 (to remove trace oxygen). For opening the reactors, for example during medium replacement, an anaerobic glovebox (Coy Lab Products, Grass Lake, MI, U.S.A.) was used that contained an atmosphere of H_2 (3% v/v) and N_2 (97%). The headspace in the reactors removed from the glovebox was then flushed with 20% CO_2 and 80% N_2 before the start of each batch cycle. The pH of the medium was adjusted to 7 before autoclaving, gassing, and addition of nutrients such as vitamins, trace elements, and bicarbonate. No further pH adjustments were made during operation of the reactors.

MMC Construction. Two-chamber reactors were used that each had a liquid volume of 100 mL and a headspace volume of 52 mL. The chambers (glass bottles, VWR, Radnor, PA, U.S.A.) were connected by side-arms with an inner diameter of 2.4 cm and a length of 3.8 cm, sealed with an O-ring, and separated by a Nafion membrane (Fuel Cell Store, Boulder, CO, U.S.A.) that was held with a screw clamp (35/25, VWR, Radnor, PA, U.S.A.). The reactor tops were sealed with rubber stoppers held tight using polypropylene screw caps with a 2.5 cm center hole (Wheaton, Millville, NJ, U.S.A.). The stoppers of the working electrode chamber (biocathode chamber) had a 4 mm

diameter hole to allow insertion of a reference electrode. The side of the inserted reference electrode was in contact with the working electrode surface.

Electrode potentials were measured using Ag/AgCl reference electrodes (−200 ± 5 mV vs SHE; model RE-5B, BASi, West Lafayette, IN, U.S.A.), and all potentials reported here were vs SHE. Reference electrodes were refurbished by placing them in 0.6 M HCl until black precipitates were dissolved and then equilibrated in 3 M NaCl saturated with AgCl in the dark until the correct offset was achieved. All reference electrodes were replaced using refurbished electrodes at the end of each batch cycle.

Electrodes and Catalysts. Carbon black powder (Vulcan XC72) was mixed 10% (w/w) with minerals (ferrihydrite, magnetite, or iron sulfide), MoS_2, or metals. The two metal powders used were stainless steel (type 316-L, Fe:Cr:Ni:Mo 67.5:17:13:2.5 wt %, particle size <44 μm) and nickel (99.8%, particle size <44 μm). Platinum was purchased 10% (w/w) premixed with carbon black (Vulcan XC72). Platinum in carbon black, steel, nickel, MoS_2, and magnetite were purchased from VWR (Radnor, PA, U.S.A.) with >99.98% purity. Ferrihydrite was prepared by neutralization of an $FeCl_3$ solution with NaOH[22] and iron sulfide by one-to-one mixing of two anaerobic solutions of 1.1 M $FeCl_2$ with 1.0 M NaS_2. Ferrihydrite and iron sulfide particles were washed once with deionized water. Iron sulfide was prepared under anaerobic conditions. After centrifugation, powders were dried for 2 d in a desiccator placed in an anaerobic glovebox.

Graphite block electrodes were used plain (Grade GM-10, GraphiteStore, Buffalo Grove, IL, U.S.A.) or coated with these minerals, metals, or carbon black (Vulcan XC72, Cabot, Boston, MA, U.S.A.). The dimensions of the electrodes were 2 cm × 2 cm × 0.32 cm. Two holes of 0.8 mm diameter drilled at a distance of 3 mm and 6 mm from the cathode edge were used to insert a titanium wire (0.8 mm diameter, 11 cm length, McMaster-Carr, Cleveland, OH, U.S.A.), providing good contact (<0.1 Ω resistance). The catalyst coating was prepared by mixing the material (10% w/w) with carbon black powder using borosilicate glass balls (3 mm diameter) and a vortexer. Deionized water (70 μL) was added, and the solution mixed again. To obtain a binding paste, 260 μL of 2-propanol and 540 μL of Nafion in an unspecified mix of alcohols (5% w/v Sigma-Aldrich, St. Louis, MO, U.S.A.) were added, and this solution was mixed again. The paste was applied to the graphite blocks using a paintbrush. All electrodes were air-dried overnight except the iron sulfide electrodes that were dried and stored in an anaerobic glovebox. By puncturing the butyl rubber sheet with the titanium wire, the electrode was fixed slightly off-center from the reference electrode.

Carbon fiber brush electrodes (4 cm × 4 cm, made from carbonized polyacrylonitrile fibers sold as "Panex 35"; Zoltek, St. Louis, MO, U.S.A.) with titanium wire cores were tested as working electrodes (cathode) and were also used as the counter electrode (anode) in all tests. A single brush had a 7×10^5 greater surface area (740 m^2) than the graphite block (10.6 cm^2) used here. Brush electrodes were pretreated by heating for 1 h at 450 °C and connected to the circuit using titanium wires.

Reactor Operation. All tests were conducted in duplicate at a given set cathodic potential or in open circuit conditions (controls). Multichannel potentiostats (MPG2, Bio-Logic, Knoxville, TN, U.S.A.) were used to set cathode potentials and recorded current in 15 min intervals. Reactors were wrapped in aluminum foil (to inhibit growth of phototrophs) and incubated at 30 °C without shaking or stirring.

Before inoculation, the reactors were incubated with fresh medium to determine abiotic hydrogen production rates. This batch cycle was cycle 0. The medium was replaced by fresh medium and inoculated. This inoculation cycle was cycle 1. The end of a batch cycle was defined as an increase in the methane concentration of less than 10% the previous measurement. Then, the catholyte was replaced by fresh medium and reinoculated with 10% reactor broth of the previous batch cycle. The anolyte was completely replaced by fresh medium. Batch cycles typically lasted for 4−5 weeks for all materials except platinum, which required 2−3 weeks per cycle except during the batch cycle following the inoculation cycle (cycle 2, Table S1, Supporting Information). During the last batch cycle, the dependence of methane formation rates on the set potential was tested by changing the potential of −600 mV to a slightly more positive (−550 mV) or more negative (−650 mV) potential. To clearly demonstrate the effect of set potentials, the better performing reactor (higher methanogenesis rate) of the duplicates was set to −550 mV, with the other reactor set to −650 mV.

Rates of gas production were calculated from a linear regression over the entire batch cycle and normalized by medium volume. Coulombic recoveries were calculated as the ratio between charge transferred and charge recovered as methane as summarized in the Supporting Information.[23]

Chemical and Electrode Analyses. Methane and hydrogen gas concentrations were measured using gas chromatography (GC). Hydrogen gas production rates results were divided by 4 to normalize them on a molar basis to methane, assuming stoichiometric conversion of 4 mols of hydrogen gas to 1 mol of methane. Concentrations of acetic, formic, propionic, and butyric acids were determined using high performance liquid chromatography (HPLC). Electrodes were prepared and examined using environmental scanning electron microscopy (ESEM). Additional information regarding these procedures is provided in the Supporting Information.

RESULTS

Methane and Hydrogen Gas Production Rates. Methane production was observed in all reactors following inoculation (batch cycle 1; Figure 1). There was no significant

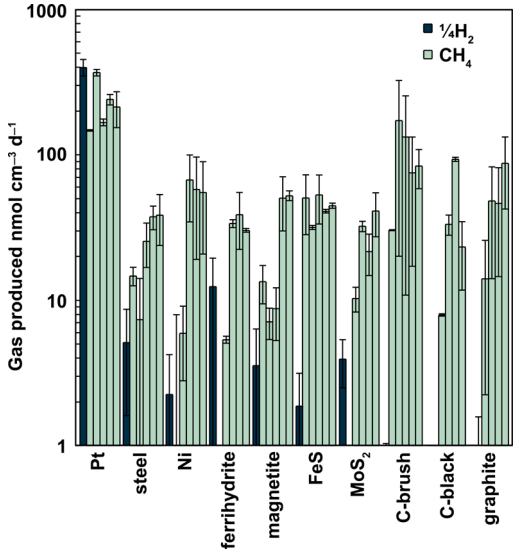

Figure 1. Rates of abiotic hydrogen formation before inoculation (dark blue, batch cycle 0) and for methane production after inoculation (light green, batch cycles 1−5, listed in sequential order for each material). Hydrogen production rates are divided by 4 to normalize production for conversion to methane (assuming 4 mol hydrogen to produce 1 mol methane). Results are presented as averages after subtraction of rates of gas production in open circuit controls, with the error bars indicating the upper and lower range of the replicate reactors.

difference between the set potential and open circuit controls during this first cycle (Student's t test, $p > 0.2$). Therefore, reactor performance for cycle 1 was excluded from subsequent analyses.

Over four cycles following microbial inoculation and acclimation, methane gas production rates with platinum (247 ± 87 nmol cm^{-3} d^{-1} equals 5.5×10^{-3} m^3 [gas] m^{-3} [medium] d^{-1}, cycles 2−5) were higher than those obtained using any other material (Figure 1). The next highest methane

dx.doi.org/10.1021/sc400520x | ACS Sustainable Chem. Eng. 2014, 2, 910−917

production rate on average was obtained using carbon brush cathodes (116 ± 117 nmol cm^{-3} d^{-1}, cycles 2–5), although relatively high rates were obtained in some cycles with plain graphite plates or those coated with carbon black. The highly variable gas production rate with the brush cathodes was due to large differences in cycle 2 for the duplicate reactors (324 nmol cm^{-3} d^{-1} and 20 nmol cm^{-3} d^{-1}). However, further acclimation reduced these differences between the two reactors (118 nmol cm^{-3} d^{-1} and 67 nmol cm^{-3} d^{-1} in cycle 5). Oxygen intrusion was detected in three poised potential reactors during cycle 2 (one iron sulfide cathode and both plain graphite cathodes; Table S1, Supporting Information). Operation of these reactors was interrupted, and an extra cycle was run to replace the compromised cycle. Despite this oxygen contamination, stable methanogenesis was established during the remaining 4 cycles.

Although the rates of methane production by the open circuit reactors (controls) were similar to those of the reactors with set potentials during the inoculation cycle, there was no evidence of methane production following this first cycle (cycle 2; Figure S1, Supporting Information). However, by cycle 5, methane was detected in several reactors including those with carbon black, carbon brush, and plain graphite cathode materials. The highest methanogenesis rate recorded under open circuit conditions occurred during cycle 5 with the ferrihydrite doped carbon black electrode (21 nmol cm^{-3} d^{-1}). Methanognesis was also observed in the graphite reactor under open circuit conditions, with the highest rate during cycle 4 of 9 nmol cm^{-3} d^{-1}.

Hydrogen gas production was measured under abiotic conditions, prior to the inoculation of the reactors (batch cycle 0) at the same set potential of −600 mV (vs SHE; Figure 1). Because reported molar hydrogen production rates were divided by 4 (Materials and Methods), the maximum possible methane production using only hydrogen is easily evaluated based on the bar heights in Figure 1. For all materials except platinum, methane rates in the final cycles were higher than those possible due to abiotic hydrogen production. Abiotic hydrogen gas production rates were the highest for platinum cathodes (1450–1750 nmol cm^{-3} d^{-1}), followed by ferrihydrite (30–70 nmol cm^{-3} d^{-1}), with all other metals and mineral-based cathodes on average producing less than 10 nmol cm^{-3} d^{-1}. Abiotic hydrogen production rates for all cathodes with carbon materials were less than or equal to 4 nmol cm^{-3} d^{-1}).

Methanogenesis at Different Set Potentials. Following cycle 5, one duplicate reactor (lower gas production rate) was set at a more negative potential of −650 mV, and the other one was set to a more positive potential of −550 mV (cycle 6). In general, all reactors had equal or improved methane production rates at the more negative potential (Figure 2), except the iron sulfide cathode that had similar methane production rates (57 nmol cm^{-3} d^{-1} at −650 mV and 55 nmol cm^{-3} d^{-1} at −550 mV). The response to a more positive potential was typically a lower methane production rate; however, there was no obvious trend with the different materials at this more positive potential. While platinum performed best at more negative potentials, at a more positive potential of −550 mV, methane gas production by plain graphite (76 nmol cm^{-3} d^{-1}) was similar to that of platinum (73 nmol cm^{-3} d^{-1}). Linear sweep voltammography conducted at the beginning of cycle 6 indicated that the biocathodes had indistinguishable overpotentials between −550 and −650 mV (Figure S2, Supporting Information).

Production of Volatile Fatty Acids. At the end of cycle 6, acetic and formic acid were detected in some reactors (no

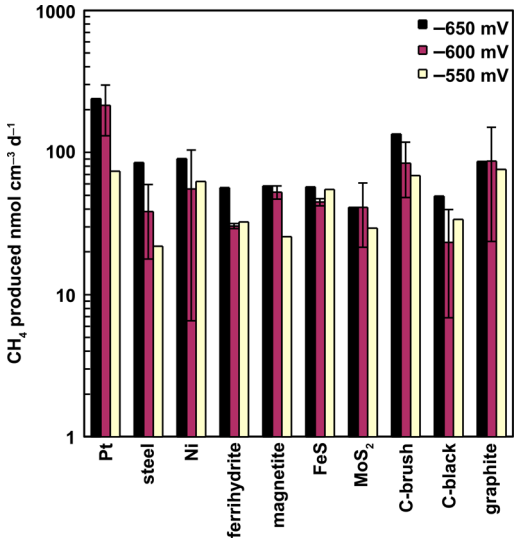

Figure 2. Effect of changing set potential from −600 mV vs SHE (average of duplicate reactors in cycle 5) to −650 or −550 mV (individual reactors split and examined in cycle 6). Error bars indicate high and low values of the duplicates during cycle 5.

detectable propionic or butyric acids in any reactors). All open circuit reactors except those with ferrihydrite and MoS_2 cathodes contained acetate (Figure 3), with formate detected

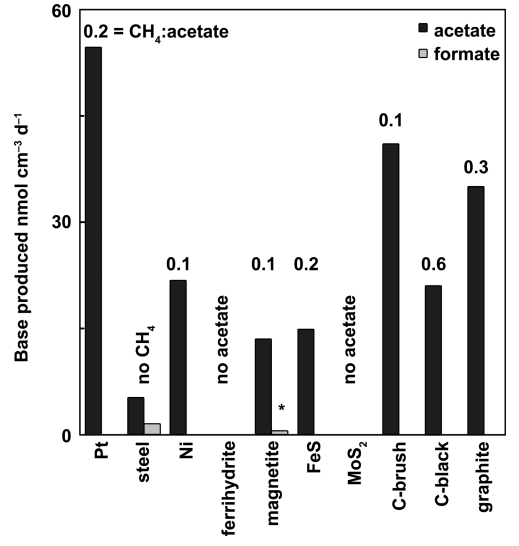

Figure 3. Acetate and formate produced in open circuit reactors. Numbers indicate the molar ratio between methane and acetate. The asterisk (*) indicates a ratio of methane:formate of 1:7 for magnetite. When no methane or no acid was produced, then the ratio could not be calculated.

only in the reactors with stainless steel and magnetite cathodes. In the poised potential reactors, only those with platinum (5 nmol cm^{-3} d^{-1}) or carbon black (17 nmol cm^{-3} d^{-1}) cathodes had recoverable formate. Acetate was detected in one of the duplicate set potential reactors with platinum (3 nmol cm^{-3} d^{-1}), nickel (7 nmol cm^{-3} d^{-1}), or carbon brush (6 nmol cm^{-3} d^{-1}) cathodes. Overall, there was little apparent relationship between the materials and organic acids recovery. In open circuit controls, there was greater acetate production than methane production, as the methane-to-acetate ratio was always less than 1 (Figure 3). In the poised potential reactors,

dx.doi.org/10.1021/sc400520x | ACS Sustainable Chem. Eng. 2014, 2, 910–917

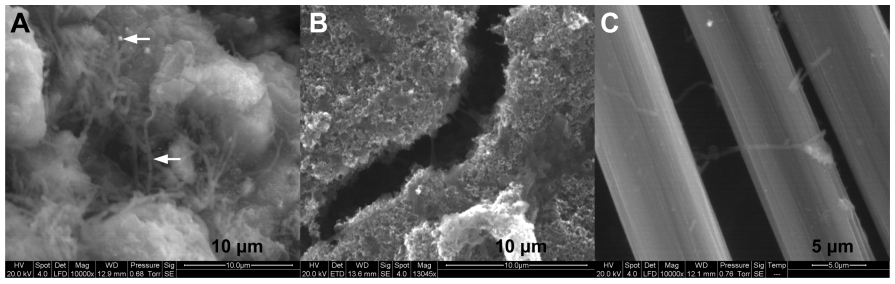

Figure 4. Scanning electron microscopic (SEM) images of cathode surfaces at poised potentials after the experiment was terminated showing the formation of microbial cell aggregates. (A) Platinum on carbon black with arrows indicating a platinum particle (top) and a microbial filament (bottom). (B) Microbial biofilms form bridges across cracks in iron sulfide doped carbon black underneath the surface. (C) Carbon fiber brush with microbial filaments.

however, opposite was seen as methane production always exceeded acetate or formate production. In the reactors where methane and acetate were produced, the methane-to-acetate ratio was 26 for platinum, 16 for the carbon brush, and 7 for nickel. In the other poised reactors, no acetate was detected. The methane-to-formate ratio was always greater than 1 in all reactors and independent from the poised potential.

Examination of the Electrodes. Biofilm formation was observed on all electrodes, although the high surface area carbon fiber brushes were more sparsely colonized than the other materials (Figure 4; Figure S3,Supporting Information). Analysis using energy-dispersive X-ray spectroscopy (EDX) of the carbon black powder mixtures confirmed the presence of the added metals and mineral particles. At the end of the experiment, particles composed of molybdenum and sulfur were present on the MoS_2 cathodes (Figure S3B, Supporting Information), but no iron was found on the iron mineral cathodes. Platinum and steel particles in the carbon black powder were identifiable after the experiment was terminated in EDX scans but not nickel. For carbon cathode materials, it was seen that microbes penetrated deeply into the applied carbon black layer (Figure 4). It appeared that extracellular polymeric substances (EPS) may have bridged cracks in the surface of the iron sulfide cathode that formed during the dehydration step of the preparation for ESEM analysis.

Coulombic Recoveries. CRs were consistently less than 100% only for the platinum cathodes, ranging from 93 ± 14% in cycle 2 to 63 ± 3% in cycle 5 (Figure 5). However, all the other materials had Coulombic recoveries that could exceed 100%. The highest Coulombic recoveries were observed for the carbon black-only reactors (1200 ± 500%, cycle 2). As the experiment proceeded, the Coulombic recoveries generally converged to values closer to 100% in all but the platinum reactors. There was substantial variability among some of the duplicate cathodes. The highest overall variability (from cycle 2 to cycle 5) was observed for the carbon brush cathodes with 286 ± 351%, while it was the lowest for the platinum cathodes, with 78 ± 15% (Figure S4, Supporting Information). The high variability was mostly due to results for cycle 2, and differences between the duplicate reactors decreased for all but the carbon black-only reactors for cycles 3−5 (Figure S4, Supporting Information). If cycle 2 is not included in these comparisons, then the iron sulfide reactors had the smallest differences (101 ± 9%) and carbon black-alone the highest variability (330 ± 392%).

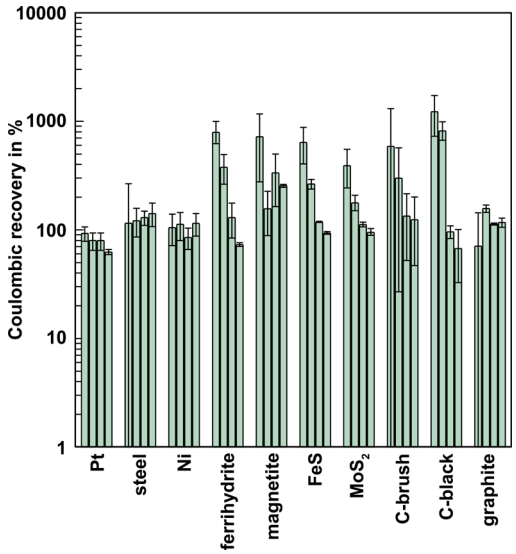

Figure 5. Coulombic recoveries in individual batch cycles (2 through 5, in order from left to right for each material). Error bars indicate upper and lower range of the replicate reactors.

DISCUSSION

In reactors containing platinum catalyst cathodes, methane was produced at a rate consistent with hydrogen production rates measured in abiotic controls. For all the other materials tested, methane rates exceeded those possible by hydrogen evolution alone. Methane production in excess of that possible by abiotic hydrogen production could be due to hydrogen evolution catalyzed by a biofilm,[24,25] methane derived from organic or inorganic materials introduced into the reactor during inoculation (either the original sludge organics or the cathode material itself), or electron transfer from the cathode to the methanogens by direct transfer or via self-produced electron shuttles. While it is possible that the presence of a biofilm enhanced hydrogen production rates in these reactors by accelerating the rate of removal of the evolved hydrogen, previous tests have shown that stirring and other methods to increase mass transfer in these systems have and little effect on hydrogen production rates under conditions where the evolution rate of hydrogen is slow.[4] Organic matter remaining from the inoculation cycle could have contributed to the high rate of methane production, especially for brushes that might capture more material than flat electrodes that have much lower surface area. One of the brush cathode reactors did have a very high rate of methane production (second only to those with

dx.doi.org/10.1021/sc400520x | ACS Sustainable Chem. Eng. 2014, 2, 910−917

platinum), but the duplicate brush cathode reactor had a much lower methane production rate. This better performing brush cathode reactor also had very high Coulombic recoveries (up to 1100%), which could indicate that methane was derived from trapped organic matter and not from the electrical circuit. However, none of the open circuit controls produced methane at rates comparable to those with set potentials. In addition, many reactors with other types of cathodes also had Coulombic recoveries in excess of 100%. Thus, it is unlikely that all Coulombic recoveries larger than 100% were due solely to organic matter carryover from the inoculation cycle. Unfortunately, the importance of direct or indirect electron transfer to methane production in these experiments could not be assessed because the methane production rates were in excess of that possible by the measured current.

The most likely reason for high Coulombic recoveries when cathodes were set at a negative potential was cathode corrosion. With methane production much greater than that possible by abiotic hydrogen production and little methane evolution in open circuit controls, the only likely source of electron donor was the cathode itself. Cathodes containing steel and nickel, which are hydrogen evolution catalysts with much higher overpotentials than platinum, had Coulombic recoveries that were only slightly above 100%. However, the iron minerals and MoS_2 cathodes had Coulombic recoveries that ranged from 99% (iron sulfide cathode) to 1030% (magnetite cathode, both in cycle 2), clearly indicating methane production in excess of that possible from current generation. The contribution of corrosion to the rates of methane production may have changed over time. For example, the Coulombic recoveries for the iron minerals and MoS_2 decreased over successive cycles from 807 ± 186% to 73 ± 3% for ferrihydrite and from 395 ± 153% to 96 ± 6% for MoS_2 (Figure 5), while methane production rates generally increased (Figure 1). An increase of Coulombic recoveries was observed only for steel (115 ± 151% to 141 ± 34%) and the plain graphite electrodes (71 ± 73% to 117 ± 11%), but note that in both cases there were large differences for the replicates in the initial cycles. The decreasing Coulombic recoveries could result from the electrodes becoming more enriched with methanogens capable of electromethanogensis, along with the rates of corrosion decreasing over time. It was not possible to quantify the relative extent that these two different processes (direct electron transfer versus corrosion) contributed to methane production for the different electrode materials. However, decreasing Coulombic recoveries (Figure 5), along with increasing methane rates (Figure 1), suggest that there was a shift away from corrosion to predominantly electromethanogenesis over time.

The possibility of cathodic corrosion has not been previously been explored in other MMC studies or those involving microbial electrosynthesis, likely because it has been assumed that the electrode materials were stable under conditions where current was flowing from the anode to the cathode. Coulombic recoveries are useful for studying the importance of corrosion in set potential reactors, but they have not always been reported.[19,26] In studies where Coulombic recoveries are given, they have usually been less than 100%. However, data are usually only reported for one cycle, often after several cycles of acclimation, and pretreatment of the cathodes and cathode materials vary. For example, Cheng et al.[4] indicated Coulombic recoveries of up to 96%. However, they did not report the number of cycles prior to this measurement, and they did not report on pretreatment of the carbon cloth electrode. Jiang et al.[18] reported that Coulombic recoveries using a carbon felt electrode (no pretreatment indicated) were less than 95% after five fed batch cycles, but they did not give results for the initial cycles when corrosion may have been more noticeable. Using reactors filled with graphite granules, Marshall et al.[15] calculated Coulombic recoveries of 84% based on measurement of several different products (acetate, formate, methane, and hydrogen) after a 10 day lag phase (5 cycles) at a set potential of −590 mV. In cycle 6, a decrease to 54% was observed, which could reflect changes in the electrode composition. In our experiments, Coulombic recoveries using graphite blocks, pretreated in a similar way to that of Marshall et al. (but without acetone and alkali washes), produced Coulombic recoveries above 100% here for all cycles at a similar set potential of −600 mV, although these recoveries declined as the experiment proceeded (Figure 5). Coulombic recoveries less than 100% do not eliminate the possibility of cathodic corrosion, only that corrosion would have been less important for methane production than that observed here.

While experiments performed here were not directed at evaluating cathode corrosion, there were other aspects of our findings that support cathode corrosion being enhanced through set potentials in the biotic experiments. In our open circuit control experiments, there was no significant methane production after the first cycle following replacement of the reactor medium, indicating no initial electrode corrosion or significant methane production from the inoculum (Figure S1, Supporting Information). However, over time there was an increase in methane in these open circuit controls, suggesting that corrosion was occurring and that it increased in response to biofilm development. Setting the cathode in the biotic tests at a low potential of −600 mV may have accelerated biofilm growth relative to open circuit controls, which could have enabled faster rates of corrosion via biodegradation of the carbon and metals compared to the controls.

Hydrocarbon impurities in the carbon black used in the metal binders, or impurities in the carbon blocks, could have provided a source of these extra Coulombs. Carbon black, which was used in the preparation of most of the cathodes, usually contains polyaromatic hydrocarbon (PAH) impurities as a result of the manufacturing process.[27] Methanogenic degradation has been well documented for aliphatic[28] and aromatic[29] hydrocarbons for decades. Two-ringed PAHs were shown to be slowly transformed into methane in mixed cultures,[30,31] and more complex PAHs are likely to follow as predicted using thermodynamic calculations.[32] While the degradation of aromatic hydrocarbons such as naphthalene to acetate and hydrogen is not thermodynamically favorable ($\Delta G^{0\prime}$ = +101 kJ mol^{-1}) under physiological standard conditions, removal of reaction products, for example, by methanogens, would make it exothermic (ΔG^0 = −90 kJ mol^{-1}) for an acetate concentration of 50 μM and H_2 = 10 Pa.[33] The negative potential needed for aromatic ring reduction of benzoyl-CoA is $E^{0\prime}$ = −622 mV,[34] which is close to that used here. It may be, therefore, that the relatively more rapid electrode corrosion was aided by the set cathode potential. Besides PAH impurities, carbon as C^0 (graphite) can be reduced to methane with hydrogen, but its oxidation to bicarbonate and hydrogen with water as electron donor is endergonic under standard conditions (Table S2, Supporting Information). Many different intermediates of methanogenic corrosion, including the hydrogenation of C^0 to aromatic rings,

dx.doi.org/10.1021/sc400520x | ACS Sustainable Chem. Eng. 2014, 2, 910−917

could have occurred. However, only the involvement of water and protons through corrosion of C^0 can thermodynamically explain the observed production of methane under open circuit conditions.

The stability of graphite blocks can be dependent on pretreatment conditions, as well as operational conditions that can affect electrode surface area and generation of precipitates. If graphite blocks were not polished, we found that the rate of hydrogen production was considerably increased. Hydrogen was produced at −600 mV by non-polished cathodes at rates between 6 and 51 nmol cm^{-3} d^{-1} and by polished cathodes at 1.30 ± 0.04 nmol cm^{-3} d^{-1}. This likely reduced the useful surface area of the graphite block. However, providing very high surface areas using carbon fiber brushes did not increase hydrogen production (Figure 1). Because hydrogen production became negligible after polishing, we conclude that impurities on the graphite blocks likely catalyzed hydrogen formation. Such impurities may be particles or mineral deposits. Metal precipitates from minerals in the medium can form on the cathodes and may also contribute to methane production via their corrosion. In one ESEM micrograph, there was evidence of various metals such as zinc, nickel, copper, aluminum, and calcium, which were all elements supplied in the medium (Figure S3B, Supporting Information).

The rates of methane production in reactors with platinum cathodes (247 ± 87 nmol cm^{-3} d^{-1}) were about 7 times smaller on a volumetric basis than those originally reported for carbon cloth by Cheng et al. (1.8 μmol cm^{-3} d^{-1})[4] for methanogensis supported primarily by direct electron transfer at −800 mV vs SHE. Marshall et al.[15] reported rates of up 7 μmol cm^{-3} d^{-1} at −590 mV vs SHE using graphite granules of an unspecified area. In our experiment, methanogenesis rates normalized to the block projected electrode area always exceeded the 0.09 μmol cm^{-2} d^{-1} at −500 mV vs SHE reported by Cheng et al.[4] At −550 mV vs SHE, plain graphite had the highest rate of methane production with 0.72 μmol cm^{-2} d^{-1} and steel the lowest with 0.21 μmol cm^{-2} d^{-1}. Platinum was comparable to graphite with 0.70 μmol cm^{-2} d^{-1}. Rates of methane obtained here, expressed on the basis of methane production per reactor volume, could likely be increased in several ways. The potential could be set at a more negative value, such as −800 mV vs SHE used by Cheng et al.[4] A higher surface area of the cathode per volume of reactor could be used for some of the materials. The higher methane production rates by Marshall et al.[15] could have been due to the higher surface area per volume of the graphite granules than the graphite plates used here. We also observed that carbon brush reactors out-performed all other reactors during cycle 5 (Figure 1). This trend might have become clearer if the experiment had been continued for a longer time. The rate of hydrogen evolution could also be maximized using catalysts for improved hydrogen evolution, such as nickel foam or steel wool.[35] However, these materials do have high overpotentials, and therefore, energy demands would be higher than with more effective catalysts such as platinum. Improved direct electron transfer to methanogens could offer a method of reduced energy input, if better electron conduction could be made between the electrodes and the microbes. Additionally, little work has been done on optimizing the inoculum for electromethanogenesis. Marshall et al.[15] compiled published data of different inocula suggesting that brewery wastewater may be the best inoculum for methanogenic MECs, but a standardized testing in this regard with respect to factors such as set potential, materials, pH, salinity, and buffer composition has never been conducted. It may be that different inocula and transfers from existing reactors could improve MMC performance, as done for electrical power generation in MFCs.[36]

The inoculation of these reactors resulted in accumulation of organics in several instances. Acetate was detected in the solution of almost all open circuit controls (Figure 3), indicating microbial activity in the absence of current generation. Homoacetogenesis (via CO_2 reduction using H_2) and degradation of cathode impurities (like hydrocarbons) could be possible reasons for acetate production. Acetogenesis from C^0 seems possible (Table S2, Supporting Information) as acetate was detected in open circuit controls (Figure 3). It remains speculative which pathway dominated in the biotic treatments. Current generation can also result in soluble organics production. Microbial acetogenesis has been demonstrated for methanogenic biofilms growing on graphite granules at −590 mV vs SHE[15] and on carbon felt cathodes at potential between −950 and −850 mV vs SHE (assuming +200 mV vs Ag/AgCl).[18] The latter study also showed that at these potentials hydrogen and methane accumulated as well, but at more positive potentials than −750 mV vs SHE, acetogenesis was not observed. Thus, current production could have resulted in some production of soluble organics, although the concentrations of these organics were low.

These results with the different cathode materials show that at set potentials of −550 to −650 mV hydrogen evolution can easily explain observed rates of methanogensis based on hydrogen production with a favorable catalyst such as platinum. However, in the absence of platinum, methane production is enhanced to different extents based on materials and surface areas. Excluding platinum, the carbon brushes showed the best performance in terms of overall methane production rates (Figure S5, Supporting Information). At a more positive potential of −550 mV, plain graphite produced methane at rates comparable to platinum (Figure 2). The use of graphite as substitute for platinum eliminates the need for this precious metal for methane gas production at more positive potentials and renders electromethanogenesis economically feasible. However, there may be microbial assisted corrosion of these cathodes that will need to be explored in future microbial methane and microbial electrosynthesis tests.

■ ASSOCIATED CONTENT

Ⓢ Supporting Information

Additional materials and methods are provided that include the calculation of the electrode potential, medium composition, details of reactor materials preparation, and further chemical and electrochemical analyses. Additional results include batch cycle times, methanogenesis results under in open circuit controls, cathode LSVs, ESEM micrographs and their respective EDX scans, Coulombic recoveries illustrating the decrease in variability over time, and gas production rates compiled from 95% confidence intervals. This material is available free of charge via the Internet at http://pubs.acs.org.

■ AUTHOR INFORMATION

Corresponding Author

*E-mail: blogan@psu.edu. Phone: +1 814-863-7908. Fax: +1 814-863-7304.

Notes

The authors declare no competing financial interest.

■ ACKNOWLEDGMENTS

We are indebted to John Cantolina of the Materials Science Center at Penn State University for help with ESEM and Hiroyuki Kashima and Yongtae Ahn for technical assistance. This research was supported by the Global Climate and Energy Program (GCEP) and by the King Abdullah University of Science and Technology (KAUST, award KUS-I1-003-13).

■ REFERENCES

(1) Gattrell, M.; Gupta, N.; Co, A. A review of the aqueous electrochemical reduction of CO_2 to hydrocarbons at copper. *J. Electroanal. Chem.* **2006**, *594* (1), 1−19.

(2) Spinner, N. S.; Vega, J. A.; Mustain, W. E. Recent progress in the electrochemical conversion and utilization of CO_2. *Catal.: Sci. Technol.* **2012**, *2* (1), 19−28.

(3) Logan, B. E.; Rabaey, K. Conversion of wastes into bioelectricity and chemicals by using microbial electrochemical technologies. *Science* **2012**, *337* (6095), 686−690.

(4) Cheng, S.; Xing, D.; Call, D. F.; Logan, B. E. Direct biological conversion of electrical current into methane by electromethanogenesis. *Environ. Sci. Technol.* **2009**, *43* (10), 3953−3958.

(5) Villano, M.; Aulenta, F.; Ciucci, C.; Ferri, T.; Giuliano, A.; Majone, M. Bioelectrochemical reduction of CO_2 to CH_4 via direct and indirect extracellular electron transfer by a hydrogenophilic methanogenic culture. *Bioresour. Technol.* **2010**, *101* (9), 3085−3090.

(6) Dinh, H. T.; Kuever, J.; Mußmann, M.; Hassel, A. W.; Stratmann, M.; Widdel, F. Iron corrosion by novel anaerobic microorganisms. *Nature* **2004**, *427* (6977), 829−832.

(7) Uchiyama, T.; Ito, K.; Mori, K.; Tsurumaru, H.; Harayama, S. Iron-corroding methanogen isolated from a crude-oil storage tank. *Appl. Environ. Microbiol.* **2010**, *76* (6), 1783−1788.

(8) Enning, D.; Venzlaff, H.; Garrelfs, J.; Dinh, H. T.; Meyer, V.; Mayrhofer, K.; Hassel, A. W.; Stratmann, M.; Widdel, F. Marine sulfate-reducing bacteria cause serious corrosion of iron under electroconductive biogenic mineral crust. *Environ. Microbiol.* **2012**, *14* (7), 1772−1787.

(9) Venzlaff, H.; Enning, D.; Srinivasan, J.; Mayrhofer, K. J. J.; Hassel, A. W.; Widdel, F.; Stratmann, M. Accelerated cathodic reaction in microbial corrosion of iron due to direct electron uptake by sulfate-reducing bacteria. *Corros. Sci.* **2013**, *66* (0), 88−96.

(10) Kato, S.; Hashimoto, K.; Watanabe, K. Methanogenesis facilitated by electric syntrophy via (semi)conductive iron-oxide minerals. *Environ. Microbiol.* **2012**, *14* (7), 1646−1654.

(11) van Bodegom, P. M.; Scholten, J. C. M.; Stams, A. J. M. Direct inhibition of methanogenesis by ferric iron. *FEMS Microbiol. Ecol.* **2004**, *49* (2), 261−268.

(12) Zhang, Y.; Merrill, M. D.; Logan, B. E. The use and optimization of stainless steel mesh cathodes in microbial electrolysis cells. *Int. J. Hydrogen Energy* **2010**, *35* (21), 12020−12028.

(13) Hall, D. S.; Bock, C.; MacDougall, B. R. The electrochemistry of metallic nickel: oxides, hydroxides, hydrides and alkaline hydrogen evolution. *J. Electrochem. Soc.* **2013**, *160* (3), F235−F243.

(14) Tokash, J. C.; Logan, B. E. Electrochemical evaluation of molybdenum disulfide as a catalyst for hydrogen evolution in microbial electrolysis cells. *Int. J. Hydrogen Energy* **2011**, *36* (16), 9439−9445.

(15) Marshall, C. W.; Ross, D. E.; Fichot, E. B.; Norman, R. S.; May, H. D. Electrosynthesis of commodity chemicals by an autotrophic microbial community. *Appl. Environ. Microbiol.* **2012**, *78* (23), 8412−8420.

(16) Villano, M.; Monaco, G.; Aulenta, F.; Majone, M. Electrochemically assisted methane production in a biofilm reactor. *J. Power Sources* **2011**, *196* (22), 9467−9472.

(17) Van Eerten-Jansen, M. C. A. A.; Heijne, A. T.; Buisman, C. J. N.; Hamelers, H. V. M Microbial electrolysis cells for production of methane from CO_2: Long-term performance and perspectives. *Int. J. Energ. Res.* **2012**, *36* (6), 809−819.

(18) Jiang, Y.; Su, M.; Zhang, Y.; Zhan, G.; Tao, Y.; Li, D. Bioelectrochemical systems for simultaneously production of methane and acetate from carbon dioxide at relatively high rate. *Int. J. Hydrogen Energy* **2013**, *38* (8), 3497−3502.

(19) Sato, K.; Kawaguchi, H.; Kobayashi, H. Bio-electrochemical conversion of carbon dioxide to methane in geological storage reservoirs. *Energy Convers. Manage.* **2013**, *66* (0), 343−350.

(20) Call, D. F.; Merrill, M. D.; Logan, B. E. High surface area stainless steel brushes as cathodes in microbial electrolysis cells. *Environ. Sci. Technol.* **2009**, *43* (6), 2179−2183.

(21) Zhang, D.; Zhu, W.; Tang, C.; Suo, Y.; Gao, L.; Yuan, X.; Wang, X.; Cui, Z. Bioreactor performance and methanogenic population dynamics in a low-temperature (5−18 °C) anaerobic fixed-bed reactor. *Bioresour. Technol.* **2012**, *104* (0), 136−143.

(22) Lovley, D. R.; Phillips, E. J. P. Novel mode of microbial energy metabolism: organic carbon oxidation coupled to dissimilatory reduction of iron or manganese. *Appl. Environ. Microbiol.* **1988**, *54* (6), 1472−1480.

(23) Logan, B. E. *Microbial Fuel Cells*; John Wiley & Sons, Inc.: Hoboken, NJ, 2008; p 300.

(24) Batlle-Vilanova, P.; Puig, S.; Gonzalez-Olmos, R.; Vilajeliu-Pons, A.; Bañeras, L.; Balaguer, M. D.; Colprim, J. Assessment of biotic and abiotic graphite cathodes for hydrogen production in microbial electrolysis cells. *Int. J. Hydrogen Energy* **2014**, *39* (3), 1297−1305.

(25) Cheng, S.; Logan, B. E. Sustainable and efficient biohydrogen production via electrohydrogenesis. *Proc. Natl. Acad. Sci. U.S.A.* **2007**, *104* (47), 18871−18873.

(26) Fu, Q.; Kobayashi, H.; Kawaguchi, H.; Vilcaez, J.; Sato, K. Identification of new microbial mediators for electromethanogenic reduction of geologically-stored carbon dioxide. *Energy Procedia* **2013**, *37* (0), 7006−7013.

(27) Qazi, A. H.; Nau, C. A. Identification of polycyclic aromatic hydrocarbons in semi-reinforcing furnace carbon black. *Am. Ind. Hyg. Assoc. J.* **1975**, *36* (3), 187−192.

(28) Muller, F. On methane fermentation of higher alkanes. *Antonie van Leeuwenhoek* **1957**, *23* (1), 369−384.

(29) Grbić-Galić, D.; Vogel, T. M. Transformation of toluene and benzene by mixed methanogenic cultures. *Appl. Environ. Microbiol.* **1987**, *53* (2), 254−260.

(30) Berdugo-Clavijo, C.; Dong, X.; Soh, J.; Sensen, C. W.; Gieg, L. M. Methanogenic biodegradation of two-ringed polycyclic aromatic hydrocarbons. *FEMS Microbiol. Ecol.* **2012**, *81* (1), 124−133.

(31) Siegert, M.; Cichocka, D.; Herrmann, S.; Gründger, F.; Feisthauer, S.; Richnow, H.-H.; Springael, D.; Krüger, M. Accelerated methanogenesis from aliphatic and aromatic hydrocarbons under iron and sulfate reducing conditions. *FEMS Microbiol. Lett.* **2011**, *315* (1), 6−16.

(32) Siegert, M.; Sitte, J.; Galushko, A.; Krüger, M. Starting up microbial enhanced oil recovery. *Adv. Biochem. Eng. Biotechnol.* **2013**, DOI: 10.1007/10_2013_256.

(33) Gieg, L. M.; Fowler, S. J.; Berdugo-Clavijo, C. Syntrophic biodegradation of hydrocarbon contaminants. *Curr. Opin. Biotechnol.* **2014**, *27* (0), 21−29.

(34) Kung, J. W.; Baumann, S.; von Bergen, M.; Müller, M.; Hagedoorn, P.-L.; Hagen, W. R.; Boll, M. Reversible biological Birch reduction at an extremely low redox potential. *J. Am. Chem. Soc.* **2010**, *132* (28), 9850−9856.

(35) Ribot-Llobet, E.; Nam, J.-Y.; Tokash, J. C.; Guisasola, A.; Logan, B. E. Assessment of four different cathode materials at different initial pHs using unbuffered catholytes in microbial electrolysis cells. *Int. J. Hydrogen Energy* **2013**, *38* (7), 2951−2956.

(36) Yates, M. D.; Kiely, P. D.; Call, D. F.; Rismani-Yazdi, H.; Bibby, K.; Peccia, J.; Regan, J. M.; Logan, B. E. Convergent development of anodic bacterial communities in microbial fuel cells. *ISME J.* **2012**, *6* (11), 2002−2013.